

Proceedings of the Second Annual LHCP

October 20, 2014

ATLAS measurements of multi-boson production

CHRISTOPHER HAYS

*On behalf of the ATLAS Collaboration,
Department of Physics
Oxford University, Oxford OX1 3RH, UK*

ABSTRACT

Measurements of electroweak gauge-boson pair-production in $\sqrt{s} = 7$ and 8 TeV pp collisions at the LHC probe self-couplings and interference effects to an accuracy of $\mathcal{O}(10\%)$ or better. ATLAS measurements of ZZ and WZ production at both center of mass energies, and of WW , $Z\gamma$ and $W\gamma$ production at $\sqrt{s} = 7$ TeV, are presented. Total, fiducial, and differential cross sections are given, along with limits on anomalous triple-gauge couplings.

PRESENTED AT

The Second Annual Conference
on Large Hadron Collider Physics
Columbia University, New York, U.S.A
June 2-7, 2014

1 Introduction

The study of vector-boson pair-production at the LHC provides important information on gauge-boson self-couplings and on QCD corrections, which are particularly relevant for Higgs boson measurements in these final states. Measurements of diboson (VV) production at ATLAS [1] generally include a cross section measured in the selected fiducial region, an extrapolation to a total production cross section, a cross section measured differentially in relevant variables, and limits on anomalous couplings.

The fiducial cross section is defined as

$$\sigma_{fid} = \frac{N_{data} - N_{bd}}{\mathcal{L}C_{VV}}, \quad (1)$$

where N_{data} is the number of observed events, N_{bd} is the number of events expected from background, \mathcal{L} is the integrated luminosity, and C_{VV} is the expected ratio of all selected events to the generated events in a relevant fiducial region. To extrapolate to the total cross section, the fiducial cross section is divided by A_{VV} , the ratio of events in the fiducial region to all generated events, and \mathcal{B} , the relevant branching ratios.

Diboson measurements probe triple-gauge couplings, which contain a charged current in the SM. The general Lagrangian terms that conserve C and P for these couplings are [2]

$$\mathcal{L}_{WWV} = ig_1^V (W_{\mu\nu}^\dagger W^\mu V^\nu - W_\mu^\dagger V_\nu W^{\mu\nu}) + i\kappa_V W_\mu^\dagger W_\nu V^{\mu\nu} + \frac{i\lambda_V}{m_W^2} W_{\lambda\mu}^\dagger W_\nu^\mu V^{\nu\lambda}, \quad (2)$$

where $g_1^{V,SM} = \kappa_V^{SM} = 1$ and $\lambda_V^{SM} = 0$ in the standard model (SM). The parameter g_1^γ is fixed to 1 by electromagnetic gauge invariance. Anomalous coupling limits are set in three scenarios: “LEP”, where $\Delta\kappa_\gamma = (\cos^2\theta_W/\sin^2\theta_W)(\Delta g_1^Z - \Delta\kappa_Z)$ and $\lambda_Z = \lambda_\gamma$, leaving three parameters; “HISZ”, where $\Delta g_1^Z = \Delta\kappa_Z/(\cos^2\theta_W - \sin^2\theta_W)$, $\Delta\kappa_\gamma = 2\Delta\kappa_Z \cos^2\theta_W/(\cos^2\theta_W - \sin^2\theta_W)$, and $\lambda_Z = \lambda_\gamma$, leaving two parameters; and “equal couplings”, where $\Delta\kappa_\gamma = \Delta\kappa_Z$, $g_1^Z = 1$, and $\lambda_Z = \lambda_\gamma$, leaving two parameters. Generally the anomalous couplings lead to a violation of unitarity, so a suppression factor of, e.g., $\lambda(\hat{s}) = \lambda/(1 + \hat{s}/\Lambda^2)^2$ is applied.

In order of increasing rate, ATLAS has measured ZZ production in four-lepton data in 7 and 8 TeV collisions; WZ production in three-lepton data at both energies; WW production in dilepton and mono-lepton data at 7 TeV; $Z\gamma$ production in dilepton-plus-photon and monophoton data at 7 TeV; $W\gamma$ production in lepton-plus-photon data at 7 TeV; and $\gamma\gamma$ production at 7 TeV.

2 ZZ cross sections

For the ZZ cross section measurements at $\sqrt{s} = 8$ TeV [3], candidate events are selected with two pairs of opposite-charge electrons or muons with invariant mass consistent with m_Z ($66 < m_{ll} < 116$ GeV). Figure 1 shows the distribution of the invariant mass of the pair with the highest dilepton p_T (the “leading” pair) versus the invariant mass of the “subleading” pair with lower dilepton p_T .

This selection provides $> 90\%$ purity, with 292.5 ± 10.6 expected ZZ events compared to a background of 20.4 ± 5.8 events in $20.3 \pm 0.6 \text{ fb}^{-1}$ of integrated luminosity. With 305 observed events, the measured total cross section $\sigma_{tot}(ZZ) = 7.1_{-0.4}^{+0.5} \text{ (stat.)} \pm 0.8 \text{ (sys.)} \pm 0.2 \text{ (lum.) pb}$ is consistent with the SM prediction ($7.2_{-0.2}^{+0.3} \text{ pb}$). The measured fiducial cross section is $\sigma_{fid}(ZZ \rightarrow llll) = 20.7_{-1.2}^{+1.3} \text{ (stat.)} \pm 0.8 \text{ (sys.)} \pm 0.6 \text{ (lum.) fb}$.

Including prior measurements, there is good agreement with SM predictions for ZZ production in hadron collisions at center of mass energies ranging from 2 to 8 TeV (Fig. 1). Measurements in pp collisions have been somewhat higher than the expectation, but not significantly so.

3 WZ cross sections

Using data corresponding to 13 fb^{-1} of integrated luminosity at $\sqrt{s} = 8$ TeV [4], candidate WZ events are selected by requiring: an opposite-charge electron or muon pair with invariant mass near m_Z ($81 < m_{ll} < 101$ GeV); an additional electron or muon; and significant missing transverse momentum ($E_T^{miss} >$

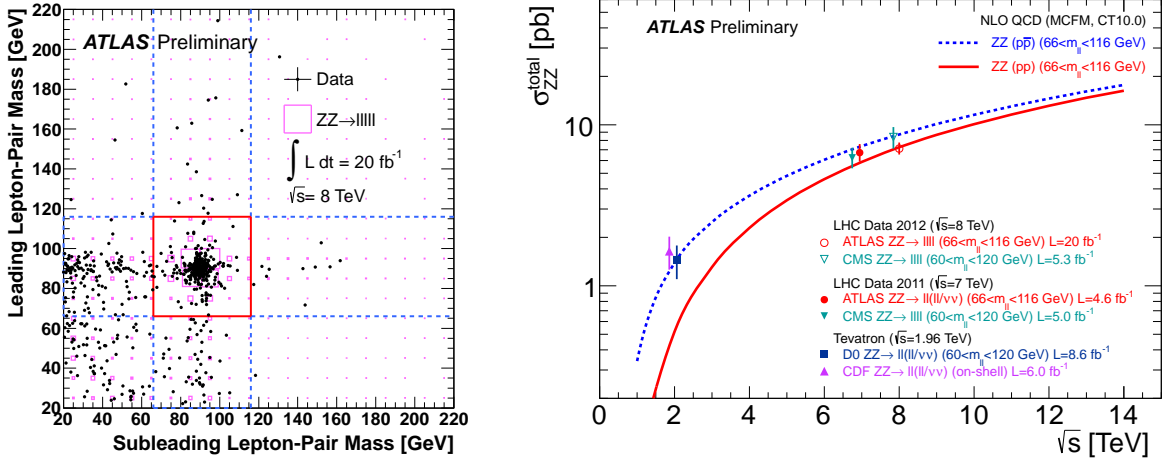


Figure 1: Left: Invariant masses of the leading and subleading lepton pairs in events with two pairs of opposite-charge electrons or muons. The leading lepton pair has higher p_T [3]. Right: The measured ZZ cross section as a function of center of mass energy for $p\bar{p}$ and pp collisions [3].

25 GeV) in a direction that is not collinear with the additional lepton ($m_T > 20$ GeV, where $m_T = \sqrt{2(E_T^\ell E_T^\nu - \vec{p}_T^\ell \vec{p}_T^\nu)}$). With this selection, the sample is 75% pure in WZ events, with 819 ± 34 expected signal events and 277 ± 26 background events. The 1094 observed events are consistent with the expectation for WZ production, as demonstrated with the m_T distribution in Fig. 2. Combining all lepton channels, the measured fiducial cross section has 7% precision, $\sigma_{fid}(WZ \rightarrow l) = 99.2^{+3.8}_{-3.0}$ (stat.) $^{+5.1}_{-5.4}$ (sys.) $^{+3.1}_{-3.0}$ (lum.) fb, and is equal to the SM expectation (99.2 ± 3.6 fb). The total measured cross section is $\sigma_{tot}(WZ) = 20.3^{+0.8}_{-0.7}$ (stat.) $^{+1.2}_{-1.1}$ (sys.) $^{+0.7}_{-0.6}$ (lum.) pb, again equal to the SM expectation (20.3 ± 0.8 pb). As with the ZZ cross section measurements, the WZ measurements are consistent with SM predictions for \sqrt{s} ranging from 2-8 TeV for $p\bar{p}$ and pp collisions (Fig. 2).

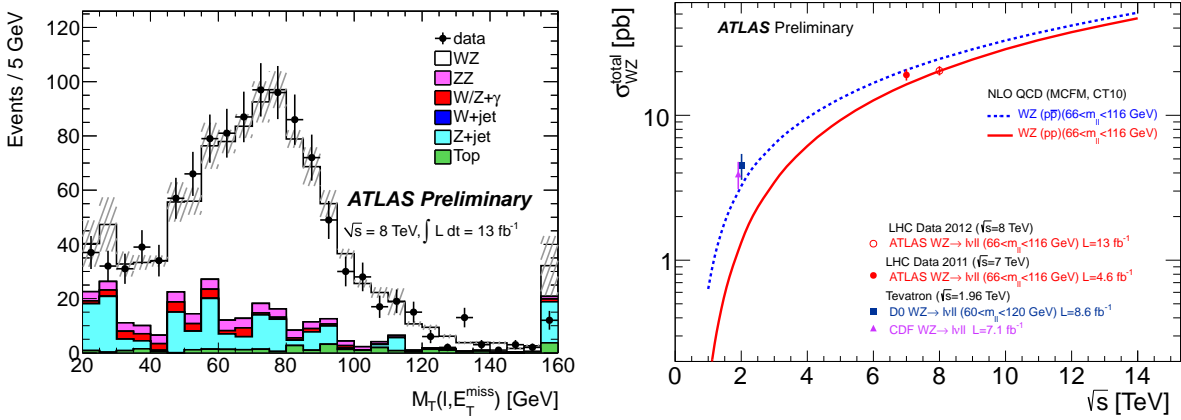


Figure 2: Left: Transverse mass m_T calculated using the lepton not associated with the Z -boson decay, and the reconstructed missing transverse momentum [4]. Right: The measured WZ cross section as a function of center of mass energy for $p\bar{p}$ and pp collisions [4].

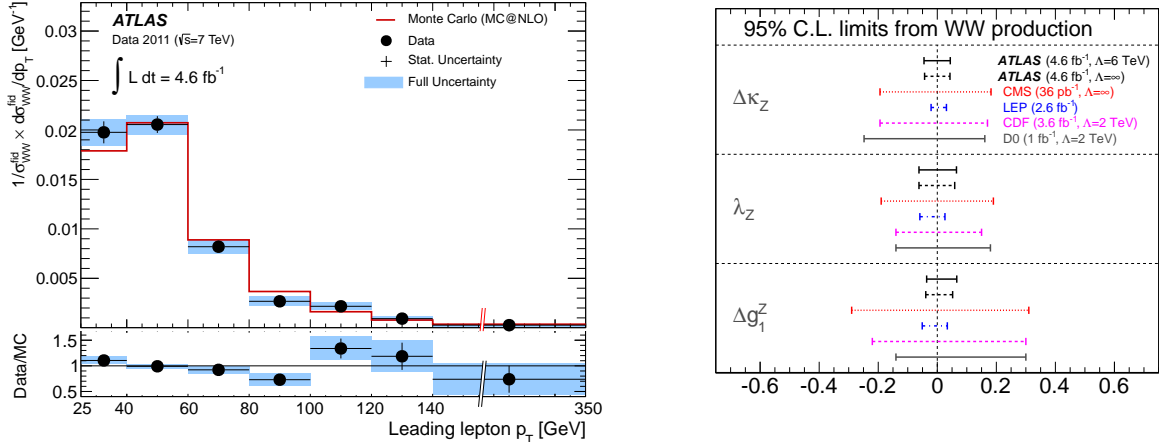


Figure 3: Left: Differential cross section for WW production as a function of leading lepton p_T , normalized by the total cross section [5]. Right: Limits on anomalous gauge couplings from the fit to the reconstructed distribution of leading lepton p_T (ATLAS), along with limits from other experiments (CMS, LEP, CDF, D0) [5].

4 WW measurements

In 4.6 fb^{-1} of $\sqrt{s} = 7$ TeV data, ATLAS has measured WW cross sections both inclusively and differentially as a function of the p_T of the highest momentum lepton in the event [5]. Events are selected with two opposite-charge leptons (electron or muon); same-flavor leptons must have invariant mass inconsistent with m_Z ($|m_{ll} - m_Z| > 15 \text{ GeV}$). The top-quark background is suppressed by requiring events to have zero jets, and Drell-Yan processes are reduced by requiring significant $E_T^{miss,rel}$, defined as E_T^{miss} multiplied by the sine of the smallest $\Delta\phi(\vec{p}_T^\ell, \vec{p}_T^\nu)$ when $\Delta\phi < \pi/2$.

The WW selection results in 824 ± 69 expected signal WW events and 369 ± 61 background events, for a purity of nearly 70%. Because of the reduced Drell-Yan background in events with different-flavor leptons, these events contain nearly two-thirds of the signal acceptance. The measured fiducial cross section in this final state is $\sigma_{fid}(WW \rightarrow e\nu\mu\nu) = 262.3 \pm 12.3$ (stat.) ± 20.7 (sys.) ± 10.2 (lum.) fb. Combining with same-flavor final states, the total cross section is 51.9 ± 2.0 (stat.) ± 3.9 (sys.) ± 2.0 (lum.) pb, which is a little more than 1σ higher than the prediction of $44.7^{+2.1}_{-1.9}$ pb.

The p_T of the lepton with the highest p_T (the “leading” lepton) probes the Q^2 of the event, and is sensitive to anomalous gauge couplings. The cross section is measured differentially as a function of leading lepton p_T , with results shown in Fig. 3. The reconstructed leading lepton p_T is fit for the presence of anomalous gauge couplings and limits are set in the absence of evidence for these couplings. Figure 3 shows the resulting limits for $\Lambda = 6$ TeV, which preserves unitarity for coupling values that are not excluded, and for $\Lambda = \infty$. Limits from prior measurements are shown for comparison.

5 $Z\gamma$ measurements

Measurements of $Z\gamma$ production have been performed by ATLAS for both $Z \rightarrow \ell\ell$ and $Z \rightarrow \nu\nu$ decays, using 4.6 fb of integrated luminosity from $\sqrt{s} = 7$ TeV collisions [6]. Events from the decay to charged leptons are selected by requiring two same-flavor leptons (electrons or muons) with invariant mass larger than 40 GeV and a photon with $p_T > 15 \text{ GeV}$. The selection yields 3990 expected signal events (with $\approx 5\%$ uncertainty) and 677 background events (with $\approx 30\%$ uncertainty), for a purity of 85%. For decays to neutrinos, the large background from photon plus jet production is suppressed by requiring a photon with $p_T > 100 \text{ GeV}$ and $E_T^{miss} > 90 \text{ GeV}$. The direction of E_T^{miss} must be opposite the photon [$\Delta\phi(E_T^{miss}, \gamma) > 2.6$] and not in the direction of a jet [$\Delta\phi(E_T^{miss}, jet) > 0.4$]. Background from W -boson production is suppressed by removing

Final state	Measured σ_{fid} (pb)	σ_{fid}^{SM} (pb)
$\ell\ell\gamma$ (≥ 0 jets)	1.30 ± 0.03 (stat.) ± 0.11 (sys.) ± 0.05 (lum.)	1.18 ± 0.05
$\ell\ell\gamma$ (0 jets)	1.05 ± 0.02 (stat.) ± 0.10 (sys.) ± 0.04 (lum.)	1.06 ± 0.05
$\nu\nu\gamma$ (≥ 0 jets)	0.133 ± 0.013 (stat.) ± 0.020 (sys.) ± 0.005 (lum.)	0.156 ± 0.012
$\nu\nu\gamma$ (0 jets)	0.133 ± 0.013 (stat.) ± 0.020 (sys.) ± 0.005 (lum.)	0.115 ± 0.009

Table 1: The measured and predicted $Z\gamma$ cross sections in the $\ell\ell\gamma$ and $\nu\nu\gamma$ final states, for events inclusive in jets and events with no jets [6].

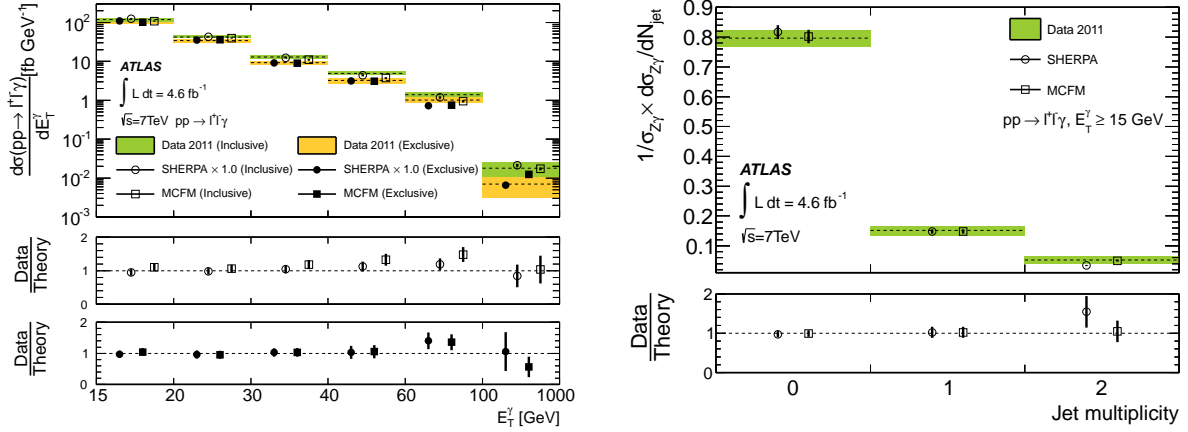


Figure 4: The differential cross sections for $Z\gamma \rightarrow \ell\ell\gamma$ production as functions of photon E_T (left) and jet multiplicity (right) [6].

events with an identified electron or muon. This selection yields 420 signal events (with $\approx 15\%$ uncertainty) and 670 background events (with $\approx 10\%$ uncertainty), for a purity of just under 40%. The purity is increased to 55% by requiring the events to have no reconstructed jets. The $Z\gamma$ measurements are performed both inclusively in jets and exclusively using events with no jets.

The measured $Z\gamma$ fiducial cross sections are consistent with the MCFM predictions, as shown in Table 1. In the $\ell\ell\gamma$ final state, the cross section is measured differentially in jet multiplicity, photon E_T , and invariant mass of the $\ell\ell\gamma$ system. Figure 4 shows good agreement between the measurement and the predictions of MCFM or Sherpa, though MCFM tends to underestimate the rate of events with photons at high E_T . These can arise from higher-order production of quarks that radiate a high-momentum photon. Sherpa is generated with tree-level diagrams of up to three additional quarks or gluons (partons), whereas MCFM has at most one additional parton in this distribution.

Events with a reconstructed photon with $E_T > 100$ GeV are used to set limits on anomalous $ZZ\gamma$ or $Z\gamma\gamma$ vertices, with limits significantly improved over those of CDF and D0 at the Tevatron.

6 $W\gamma$ measurements

The highest rate of diboson production is $W\gamma$, producing more than 10000 signal events after event selection. The selection requires an electron or muon, a photon, and large E_T^{miss} , giving a purity of $\approx 60\%$. As with the $Z\gamma$ measurements, fiducial cross sections are measured inclusively in jets and in events with no reconstructed jets (Table 2). The measured inclusive cross section is more than 2σ higher than the MCFM prediction, due to the upper limit of one additional partons produced by MCFM. The agreement with MCFM is improved in events with no reconstructed jets, though the cross section measurement is still higher than the prediction. The differential cross section with respect to photon E_T (Fig. 5) shows a discrepancy with MCFM that increases with increasing photon E_T , as with the $Z\gamma$ measurement.

Final state	Measured σ_{fid} (pb)	σ_{fid}^{SM} (pb)
$\ell\nu\gamma$ (≥ 0 jets)	2.77 ± 0.03 (stat.) ± 0.33 (sys.) ± 0.14 (lum.)	1.96 ± 0.17
$\ell\nu\gamma$ (0 jets)	1.76 ± 0.03 (stat.) ± 0.21 (sys.) ± 0.08 (lum.)	1.39 ± 0.13

Table 2: The measured and predicted $W\gamma$ cross sections in the $\ell\nu\gamma$ final state, for events inclusive in jets and events with no jets [6].

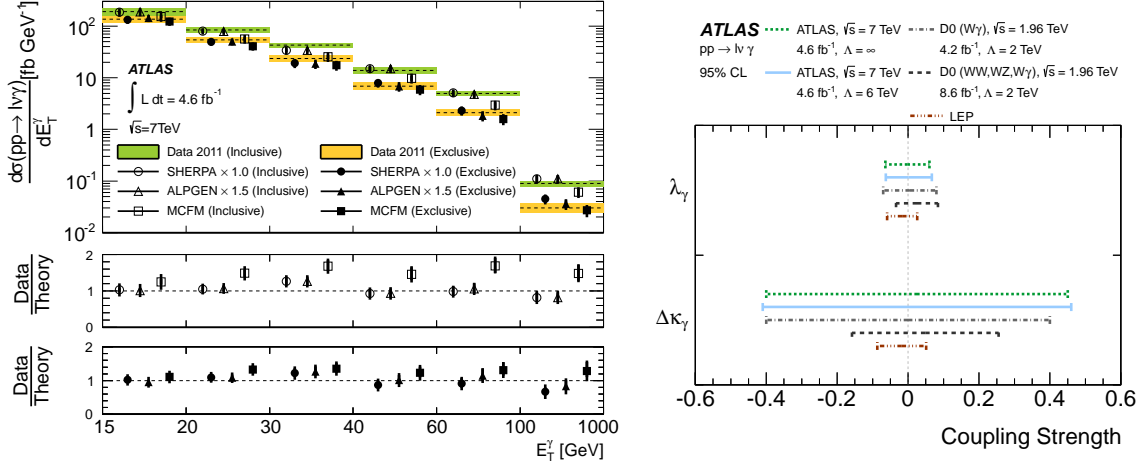


Figure 5: Left: The differential $W\gamma \rightarrow \ell\nu\gamma$ cross section as a function of photon E_T [6]. Right: Limits on anomalous couplings compared to those from D0 and LEP [6].

Anomalous couplings are probed using events with photon $E_T > 100$ GeV. The resulting limits on λ_γ and $\Delta\kappa_\gamma$ are shown in Fig. 5 for $\Lambda = 6$ TeV and $\Lambda = \infty$, assuming all other couplings have their SM values.

7 Summary

ATLAS has measured diboson cross sections in $\sqrt{s} = 7$ and 8 TeV, including a number of unfolded differential cross sections. The cross sections are sensitive to higher order perturbative QCD predictions, and demonstrate the importance of including multiple partons in the predictions. Anomalous coupling limits have been set using the results from $\sqrt{s} = 7$ TeV data.

References

- [1] ATLAS Collaboration, 2008 JINST 3 S08003.
- [2] K. Hagiwara, R. D. Peccei, D. Zeppenfeld, and K. Hikasa, Nucl. Phys. B **282** (1987) 253.
- [3] ATLAS Collaboration, ATLAS-CONF-2013-020 (2013), <https://cds.cern.ch/record/1525555>.
- [4] ATLAS Collaboration, ATLAS-CONF-2013-021 (2013), <https://cds.cern.ch/record/1525557>.
- [5] ATLAS Collaboration, Phys. Rev. D **87**, 112001 (2013).
- [6] ATLAS Collaboration, Phys. Rev. D **87**, 112003 (2013).